Exploration of a Hexagonal Structure on Saturn's Northern Pole

Tianlu Yuan

University of Colorado Boulder

Abstract

Images from Voyager revealed a hexagonal structure near Saturn's northern pole at $\approx 77^\circ$ north planetographic latitude. Ground based observations and images from the Hubble Space Telescope (HST) in the early 90s, along with Cassini data from recent years confirm that the structure still exists and appears relatively unchanged. Over the decades spanning its discovery, several theoretical descriptions of the phenomena have been offered. Allison et al. proposed a Rossby wave model sustained by perturbative forcing from a nearby vortex [2]. A more recent model by Barbosa Aguiar et al., based on barotropic instabilities caused by jets to the north and south of the hexagon's zonal flow, supported theory with experimental results by producing polygonal shapes in fluid flows within the laboratory [1]. Numerical simulations confirming this theory to an extent were also conducted [12]. Here, I present an overview of the observational data collected on the Saturnian north polar hexagon. I also discuss the two theoretical models that were put forth to explain the cause of its six-sided structure and their correctness in light of new observational data and experimental results.

I. INTRODUCTION

In the 1980s images of Saturn taken by Voyager led to Godfrey's surprising discovery of a hexagonal structure on the planet's north pole [9]. Now, over three decades later, Saturn's north polar hexagon remains, superficially unchanged and not entirely understood. Voyager's iconic images proved a challenge to explain theoretically, but with additional data from ground based observations and the HST in the early 90s, and images from the Cassini mission more recently, our knowledge of many physical parameters forming the hexagon has increased. Along with observation, laboratory experiments and numerical simulations have helped foster greater understanding of the possible causes of the jet's six-sided shape.

This paper first details the discovery of the hexagon by Godfrey and his initial measurements of the structure's velocity field and rotation rate [9, 10]. A brief discussion of ground based and HST observations follow that support the earlier velocity measurements [5, 15]. I next provide a theoretical description of the hexagon as a stationary Rossby wave, suggesting that its overall structure is sustained by perturbations from a nearby vortex observed in the Voyager images [2]. Finally, I discuss recent observational and experimental data and a different theoretical treatment of the hexagon based on barotropic instability theory [1, 3, 6, 12]. I also give a basic overview of some important fluid dynamic concepts in the appendix. Much of the technical terminology can be found there. I hope that this provides some intuition for understanding the theory, but a full, mathematical treatment of advanced concepts will be skipped.

II. DISCOVERY AND INITIAL MEASUREMENTS

The series of images of Saturn taken by Voyager 1 and 2 were mainly of Saturn's equatorial region. In order to visualize the north pole, Godfrey accounted for the spherical distortion effect by polar projecting the equatorial images and stitching them together as seen in Figure 1. He discovered a hexagonal structure at 77° that appeared to be moving at $6.3 \pm 8 \times 10^{-8}$rad/s relative to the Saturnian Radio (SR) rotation period [9]. The SR period is thought to be due to Saturn's magnetic field, which in turn reflects conditions within the conductive interior of the planet. Hence, it is believed to give an accurate measure of the rotation rate of Saturn's interior and indicates that the hexagon is stationary relative to

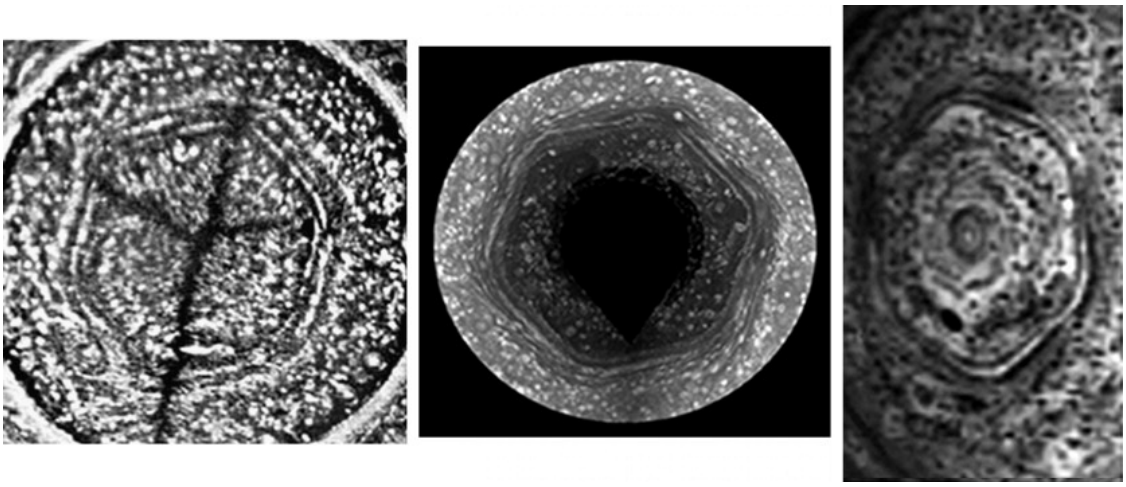

FIG. 1: Images of the Saturn polar hexagon as viewed by Voyager (left), Cassini-ISS (middle), and Cassini-VIMS (right). The impinging vortex is visible along the bottom left edge of the Voyager-taken image [12, fig 1].

Saturn's interior rotation within uncertainties [9]. For the rest of this paper, all quoted velocites will be relative to the SR rotation.

Along with the hexagon, a large anticyclonic vortex along one of the edges of the hexagon can be seen in Figure 1, and its movement was associated with that of the hexagon itself [9, 12]. In a follow-up paper, Godfrey assumed the rotation rate of the hexagon to be equivalent to that of the vortex. By measuring the relative velocity of the vortex, he concluded the rotation period of the polar hexagon to be $-8.13 \pm 0.52 \times 10^{-9}$rad/s, again suggesting an association between the hexagon and the planet's interior [10].

By tracking invidual cloud features within the hexagon, Godfrey measured the mean zonal velocity of the flow at the center of the hexagon to be ≈ 100m/s [9]. This result is a measure of the latitudinal velocity averaged over a zonal region via a nearest neighbor fit routine. Eastward movement was taken to be positive. The mean zonal velocity falls off moving latitudinally away from the center of the hexagon such that the the flow drops to ≈ -20m/s to the south and ≈ 10m/s to the north [9]. A latitudinal profile of the mean zonal velocity indicates an approximately Gaussian distribution as indicated in Figure 5. This velocity profile would prove to be important for theoretical treatments of the hexagon and will be a focus of discussion later [1, 2, 12].

Apart from the two Voyager flybys, observations of Saturn with ground based instruments and the HST served to confirm Godfrey's earlier analyses. Using a 1.05m diameter

telescope at Pic-du-Midi Observatory, a group led by Sanchez-Lavega observed Saturn's north pole over a period from July 1990 to December 1991 [15]. During this time, Saturn held a favorable orientation relative to Earth that allowed views of the polar hexagon and the associated vortex. The vortex's central longitude and latitude were measured and by combining the Pic-du-Midi data with Voyager's, a mean rotation rate of -1.17×10^{-8}rad/s over the 11 year period was cited [15]. Over a similar time period, the HST also took several images of Saturn's polar region. Focusing on measuring the position of the center of the vortex accurately, Caldwell's group defined the center of the planet as the center of the ellipse defined by Saturn's rings [5]. This was repeated for each image, and the longitude and latitude of the center of the polar spot was determined with high accuracy. A long term drift rate of -1.15×10^{-8}rad/s was reported, in fair agreement with both Godfrey's and Sanchez-Lavega's measurements [5]. It should be noted that all three measurements cited the uncertainty in the Saturnian rotation period as a possible systematic in their calculations. Nevertheless, the agreement between Voyager, Pic-du-Midi, and the HST data strongly indicated that the hexagon was both a stationary and long term feature on Saturn.

III. EARLY HYPOTHESES

The Voyager observations led Godfrey to discuss four possible causes of the stationary rotation rate of the hexagon [9]. First, stated as being unlikely, is that the rotation rate could just be a coincidence, since a stationary rotation rate is as good as any other. Another possibility is forcing, from either above or below, corresponding to Saturn's rotation, that creates the hexagonal wave. The third possibility regarded the hexagon as an aurora instead of cloud patterns, and the fourth that the radio rotation rate of Saturn is actually being generated by the hexagon instead of the planetary interior [9]. Aside from the second, these theories all seem fairly far fetched, which is understandable considering the amount of data existing at the time. The third suggestion is easily refuted by Cassini imaging data [3], while the fourth would require a direct connection between the hexagon and Saturn's magnetic field. If we assume that the hexagonal features are clouds, they would have to be ammonia crystals that could only occur within the troposphere, not the ionosphere, and its low conductivity would be unlikely to affect the magnetic field [7].

The second possibility of forcing can be divided into either forcing from below or forcing

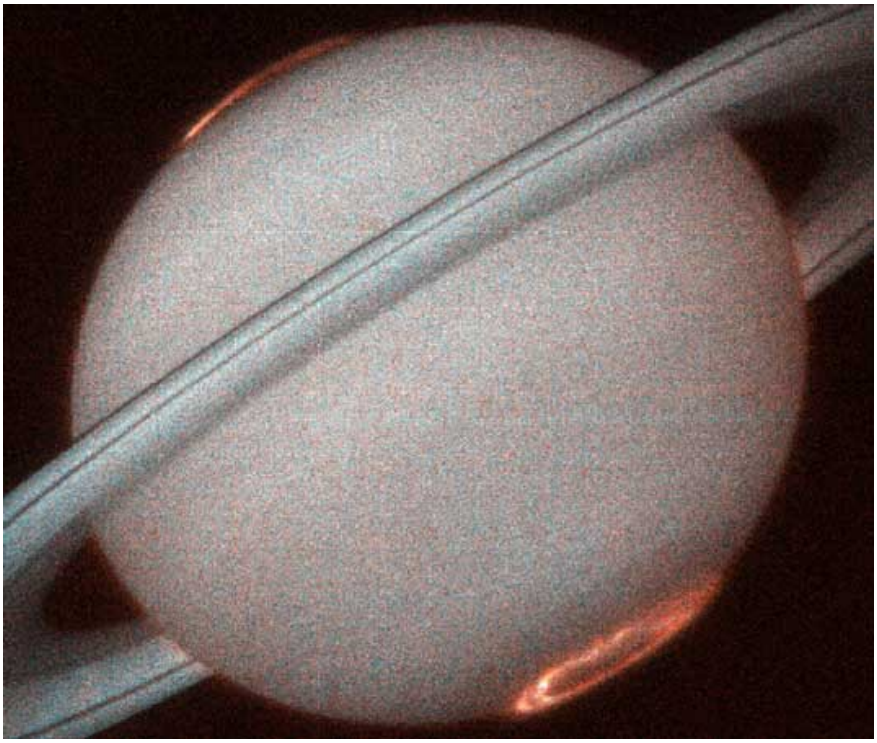

FIG. 2: Credit J. Trauger (JPL), NASA, [16]. Image of Saturn's polar UV-aurora taken by the HST.

from above. Godfrey maintains that forcing from above could be due to aurora features close to the hexagon [9]. However, this would suggest that there exists a similar hexagon in the Southern region due to symmetrical north-south aurora patterns as seen in Figure 2. Images from Cassini, Figure 3, again show that this is not the case [6]. Further, the atmospheric depth of the hexagon and its seasonal independence strongly suggests that solar effects are not its cause [3]. Forcing from below seems to be the last realistic hypothesis. Gierasch supported this theory by positing thermal convection from the interior as the cause of the stationary hexagon [7]. The limited data on Saturn's interior, however, constrains this interpretation to opinion, not fact.

IV. THE ROSSBY WAVE THEORY

The first mathematical description of Saturn's hexagon was the Rossby wave theory offered by Allison, Godfrey, and Beebe [2]. Rossby waves are large scale planetary waves characterized by low frequency modes and a non-zero Coriolis parameter [13, 14]. It is typi-

cally used in studies of large-scale, low-frequency waves in Earth's atmosphere, but Saturn's hexagon also exhibits its properties [2]. The large planetary scale of Saturn's hexagon, as well as its westward drift relative to the mean background zonal flow are distinguishing features of Rossby waves [14]. With regards to its westward phase drift, recall that the hexagon appears stationary while the jets within move at high velocities eastward, this is allowed by the Rossby wave dispersion relation (a measure of the wave velocity), given in Equation 1, which indicates that stationary waves can exist if $U > 0$ [14]. Finally, it completes six patterns about a latitudinal region, thus its wavenumber is six.

Two factors contribute to the restoring force of Rossby wave oscillations. First, the gradient of the planetary vorticity as defined by Equation A.3, $\beta = 2\Omega\cos(\theta)/a$, where Ω is the planetary rotation rate, a its radius, and θ the latitude. Second, the negative curvature of the mean zonal flow in the meridional (y) direction, $-u_{yy}$ [2]. This can be thought of as the gradient of the relative vorticity discussed in the appendix. The hexagon's zonal velocity profile can be modeled as a Gaussian function of the meridional distance from center [2]. In the β-plane approximation, which takes a latitudinal strip around a sphere and approximates it as a plane, simplifying the spherical geometry into a planar geometry [14], it can be shown that the planetary vorticity gradient is negligible. First note that the $1/e$ distance, L_e, from the mean in our Gaussian velocity profile is $\approx$ 1800km [2]. In the β-plane approximation, for latitudes within this L_e region the total vorticity gradient is dominated by the mean zonal flow [2]. Intuitively, this is because a Gaussian bell curve has maximal negative curvature near its mean. The hexagon's velocity profile is well-modeled by a Gaussian as seen in Figure 7, and thus the planetary vorticity gradient can be neglected in the Rossby wave model [2].

These approximations allows the calculation of the Rossby phase speed for barotropic waves (a brief exposition of barotropic fluids can be found in the appendix) [2],

$$c = U - \langle -U_{yy} \rangle_e \left(\frac{r}{n}\right)^2. \tag{1}$$

Here, c is the *horizontal* phase velocity, n the zonal wave number, and r the radius of the latitudinal circle, and U is our Gaussian velocity profile [2]. For the hexagon, $r \approx 1.4 \times 10^7$m, $U \approx 100$m/s, $\langle -U_{yy} \rangle_e \approx 2.2 \times 10^{-11}\text{m}^{-1}\ \text{s}^{-1}$ and $n = 6$, giving $c \approx 0$ as expected for a stationary wave [2]. However, it is important to note that this approximation neglects the vertical structure of the wave and its strict meridional confinement [2]. Nevertheless, the vertical structure can be constrained such that the resulting wave equation has a solution.

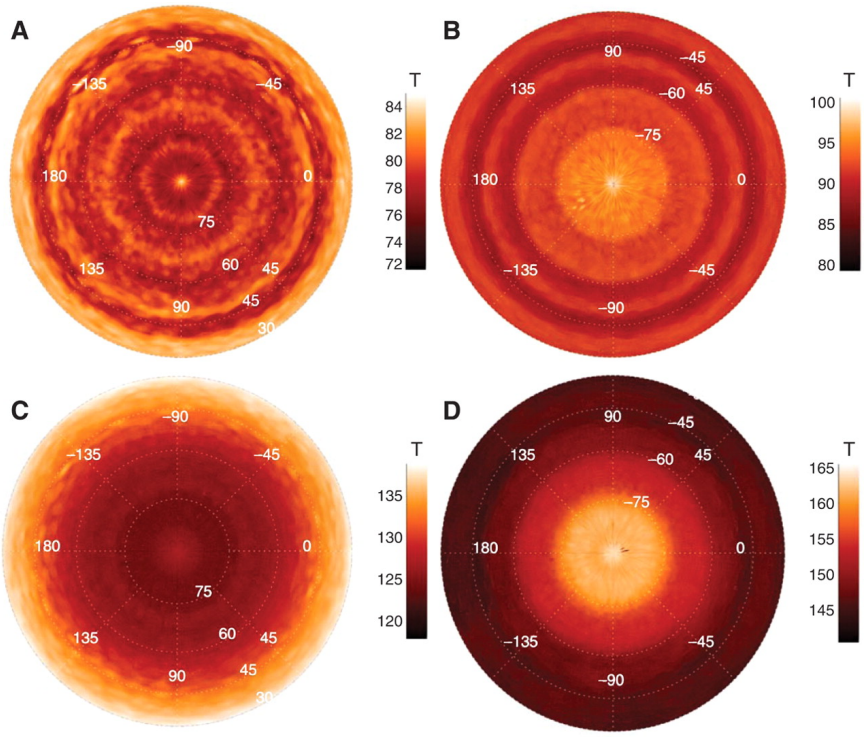

FIG. 3: Saturn's polar temperatures as captured by CIRS. The northern hemisphere is on the right, the southern hemisphere on the left. **A** and **B** are at an altitude of 100 mbar in the troposphere, **C** and **D** at 1 mbar in the stratosphere [6, fig 1].

This solution includes a perturbation term, which is assumed to be the stationary vortex impinging on one side of the hexagon [2]. Furthermore, assuming a vertically trapped wave with a vertical structure that is related to the zonal wave number in a specific manner, it can be shown that the meridional confinement of the hexagon is due to this pertubation [2].

Although Saturn's vertical structure is not well understood, based on studies of Earth's atmosphere we know that vertically trapped, stationary waves can be forced from below by internal heating [2]. This effectively sets a lower boundary condition that is dependent on thermal variations in the vertically stratified layers of the atmosphere. It is consistent with the possibility of internal forcing as suggested by Gierasch [7]. While the Rossby wave model describes the hexagon well phenomenologically, new data from the Cassini mission illustrates that the hexagon's structure cannot be due to the impinging vortex.

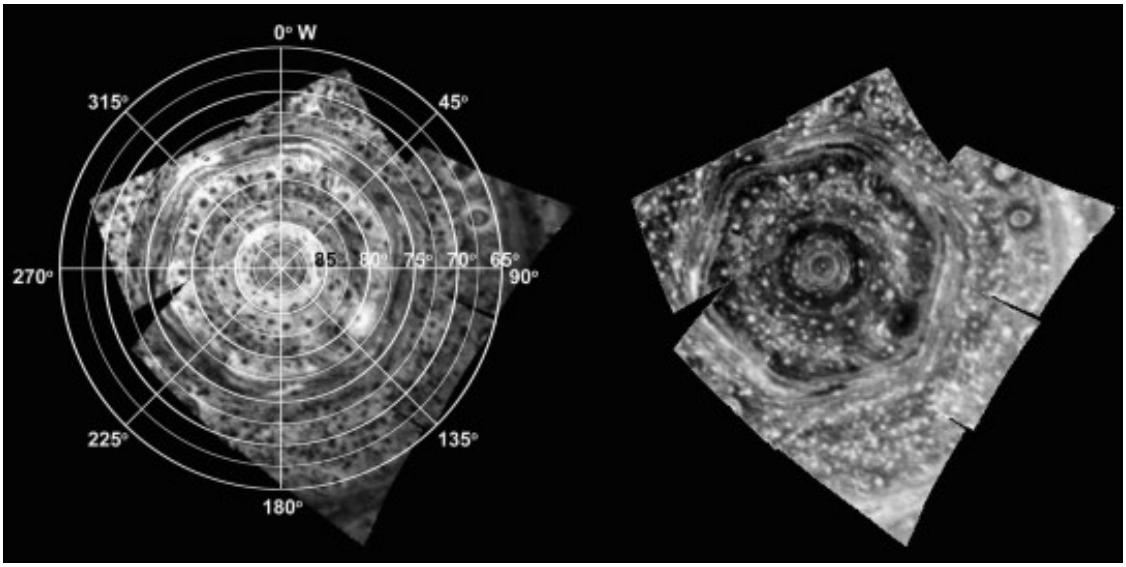

FIG. 4: Polar projection of nine 5.1μm images of Saturn's north pole. Images were obtained in darkness, thus clouds are seen as dark in the left images as they block Saturn's 5.1μm thermal emission. The photometrically inverted image on the right shows clouds as bright [3, fig 1].

V. OBSERVATIONS BY CASSINI

In 2007 the Cassini probe orbited Saturn at a high latitudinal inclination and provided the first close-up images of Saturn's poles since Voyager. Although the northern pole was shrouded by the seasonal tilt, the Cassini Composite Infrared Spectrometer (CIRS) took images of both the north and south poles at mid-infrared wavelengths [6]. It thus revealed the polar thermal distribution seen in Figure 3, and verified the existence of Saturn's north polar hexagon. Similar ephemeral polygonal waves were seen in the south polar region, but none displayed the permanence of the north polar hexagon [6]. Notably, the CIRS images did not contain any resemblance of the impinging anticyclonic vortex as seen in earlier studies [6].

Images taken by the Cassini Visual-Infrared Mapping Spectrometer (VIMS) at 5.1μm are displayed in Figure 4. Again, no evidence of the impinging vortex was observed [3]. Zonal wind profile measurements were made using VIMS images and cloud-tracking methods. The results are displayed in Figure 5, and a maximum mean zonal wind velocity of 124.5 ± 8.7m/s was recorded [3]. An analysis conducted assuming constant absolute vorticity as a function of latitude showed disagreement between expected and observed mean zonal wind profiles.

In two dimensional fluids, absolute vorticity tends to be conserved, but in three dimensions it is the potential vorticity, defined in Equation A.5, that is conserved under the conditions given in the appendix [13]. Cassini thermal measurements combined with results from the zonal velocity profile measurements gave a mean potential vorticity value as a function of latitude. The results showed that there is a step in potential vorticity at the hexagon's latitude [3].

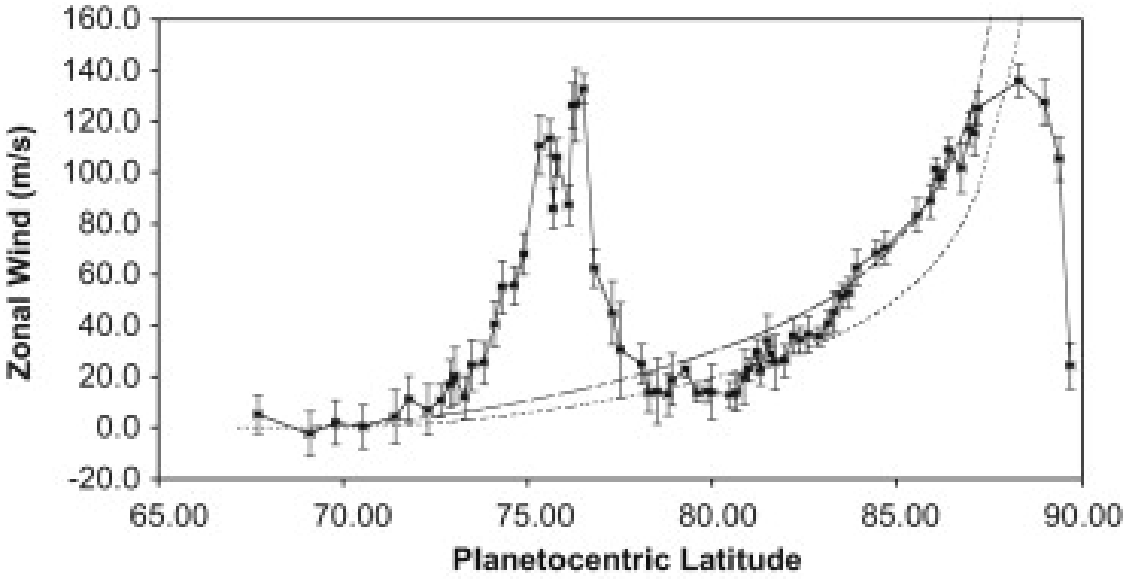

FIG. 5: Mean zonal velocity profile with Cassini data. The dashed and dotted lines are model wind velocities assuming a constant absolute vorticity. Eastward is taken to be positive along the vertical axis [3, fig 3].

The disappearance of the impinging vortex indicates that the perturbative Rossby wave theory cannot be correct [6]. Additionally, the fact that the hexagonal structure exists deep into the troposphere and seems unaffected by seasonal variations rules out solar effects on the formation of the hexagon [3]. Finally, the disagreement between the hexagon's velocity profile and the velocity profile expected from a constant absolute vorticity indicates that the third, vertical dimension plays a crucial role the formation and stability of the hexagon. Further, potential vorticity non-conservation indicates that one or more of the conditions listed in the appendix does not apply to the hexagon. This hints that a new theoretical approach is needed to describe the hexagon. Experimental and numerical studies of polygonal flows arising from barotropic instabilites are one such alternative [3].

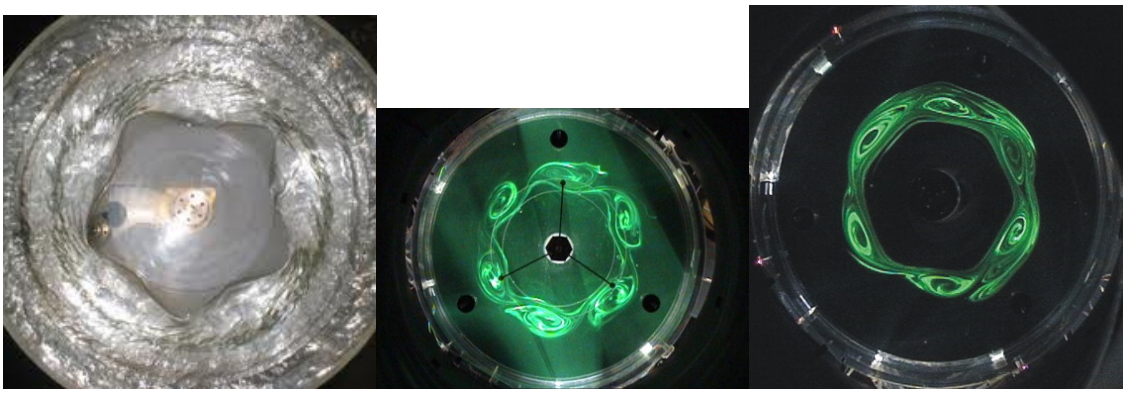

(a) Pentagon [11] (b) Ring setup [1] (c) Disk setup [1]

FIG. 6: Polygons in rotating fluid flow experiments. In (a) the experimental apparatus is a partially filled cylinder with a rotating bottom [11]. The other two figures are taken from [1, fig 9,10] and show results from the two experimental setups used by Barbosa Aguiar.

VI. LABORATORY AND NUMERICAL STUDIES

Rotating polygonal fluid flows have been created in several laboratory environments. One study by Jansson et al. demonstrated that stable polygons can be driven by the rotating bottom plate of a partially filled cylinder [11]. They speculate that this symmetry breaking is triggered by the minute wobbling of the bottom plate [11]. Another study led by Barbosa Aguiar cited barotropic instabilities in the surrounding zonal jets of the hexagon to be the driving force behinds its polygonal structure [1]. Barotropic instability can arise from horizontal shear forces in the flow, which convert kinetic energy of the zonal flow into kinetic energy of the resulting eddies [1, 13]. Using two different experimental setups, they generated polygons in a rotating fluid as seen in Figure 6, and demonstrated the existence of surrounding barotropically unstable regions similar to those measured around Saturn's hexagon [1]. A third numerical simulation also cites zonal jet instabilities as a direct link in the production of a stable polygon flow [12]. These experimental results are worth elaborating. Their analyses leads to the conclusion that Saturn's hexagon might well arise from similar flow instabilities as the polygons in Earth's experiments.

In the experiment by Jansson et al. the constraint parameters were the rotating velocity of the bottom plate and the height of the fluid. Two different fluids were tested, ethyl alcohol and water, and both exhibited rotating polygon formation [11]. The rotation rate of

the polygons were all found to be much less than the rotation rate of the bottom plate, and the number of sides of the formed polygon increased with rotation frequency and decreased with fluid height [11]. They attributed this spontaneous axial symmetry breaking to the wobbling of the bottom plate.

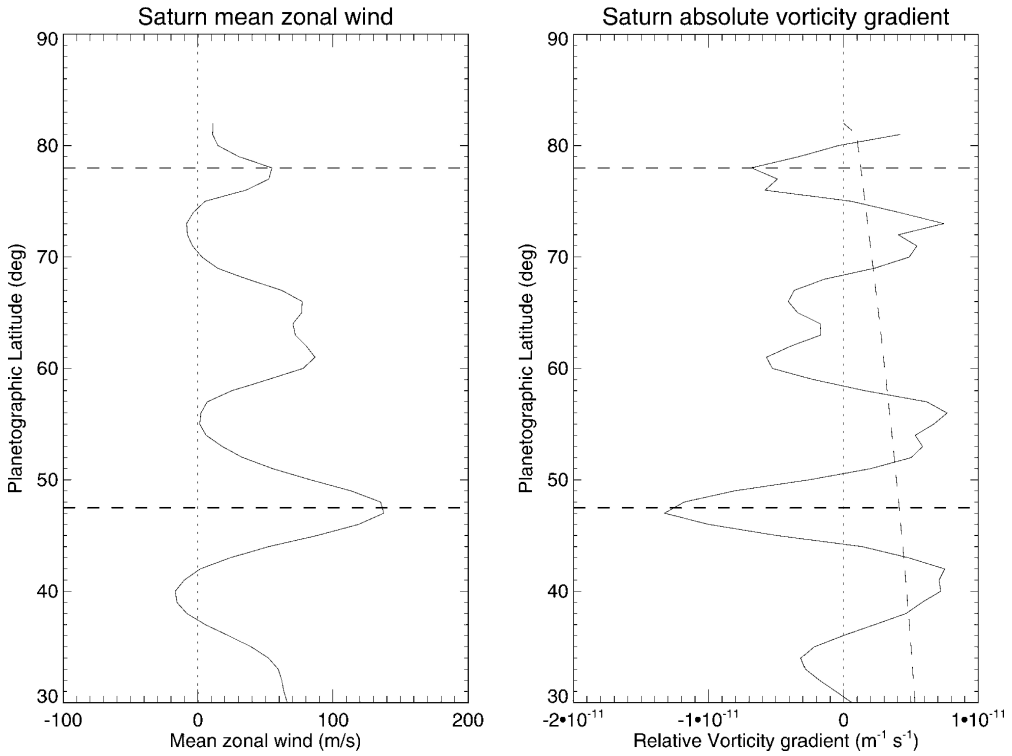

FIG. 7: From [1, fig 1]. Voyager measured zonal velocity profile and Saturn's vorticity gradient as a function of latitude. The horizontal dashed line at $\approx 77°$ correspond to the hexagon. On the right plot, the dashed line correspond to β, the solid line u_{yy}.

A more direct analogue experiment to Saturn's hexagon involved testing the assumptions of barotropic instability as a possible cause of the hexagon. A necessary condition of barotropic instability is the Rayleigh-Kuo criterion,

$$\beta - u_{yy} < 0, \tag{2}$$

where $\beta = df/dy$ and u_{yy} is the curvature of the zonal velocity profile along the northward direction [1]. As seen in Figure 7, the Rayleigh-Kuo criterion is violated on either side of the hexagon's latitude at $\approx 77°$ [1]. However, satisfying the Rayleigh-Kuo criterion alone is not sufficient for barotropic instability. If it were, one might wonder as to why no polygonal shape occurs in the southern polar region or anywhere else on Saturn for that matter.

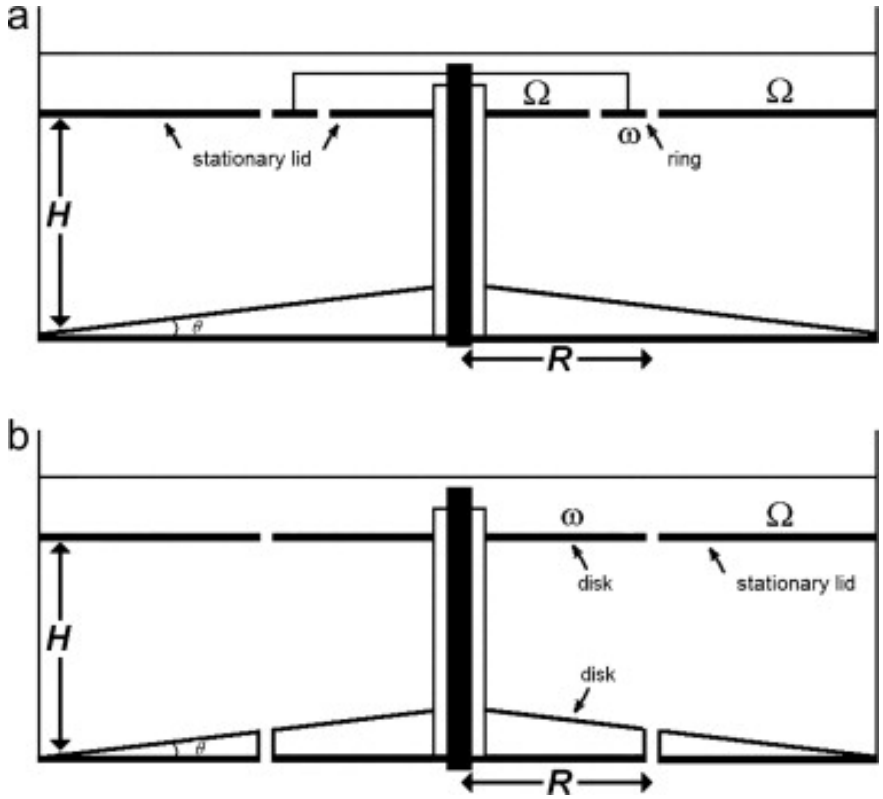

FIG. 8: The setup of the laboratory experiment conducted by Barbosa Aguiar et al. Two differentially-rotating sections were employed, a ring and a disk, to force out a zonal jet profile [1, fig 4].

After all it seems that the Rayleigh-Kuo criterion is violated in several regions of latitude below the hexagon. A theoretical model based upon a linearised barotropic equation was solved for a measured, Saturnian zonal velocity profile and several radii of deformation, L_D [1]. The Rossby radius of deformation can be intuitively thought of as the horizontal length scale at which rotational effects (e.g. Coriolis force) become as important as buoyancy effects (e.g. gravity) [8]. The solution to the linearised barotropic equation gave the wavenumber of maximal growth rate as a function of L_D. In the case of a wavenumber of 6, the corresponding L_D was found to be 2500km, whereas L_D for a jet at the hexagon's latitude is estimated to be 1135km [1, 12]. In the case of southern polar jets, solutions were found to peak at infinite wavenumbers [1].

In order to investigate this topic further, a laboratory model was developed using the two slightly differing setups shown in Figure 8. Both involved cylinders rotating at Ω, but the distinguishing feature is the separate differentially-rotating section [1]. This section could

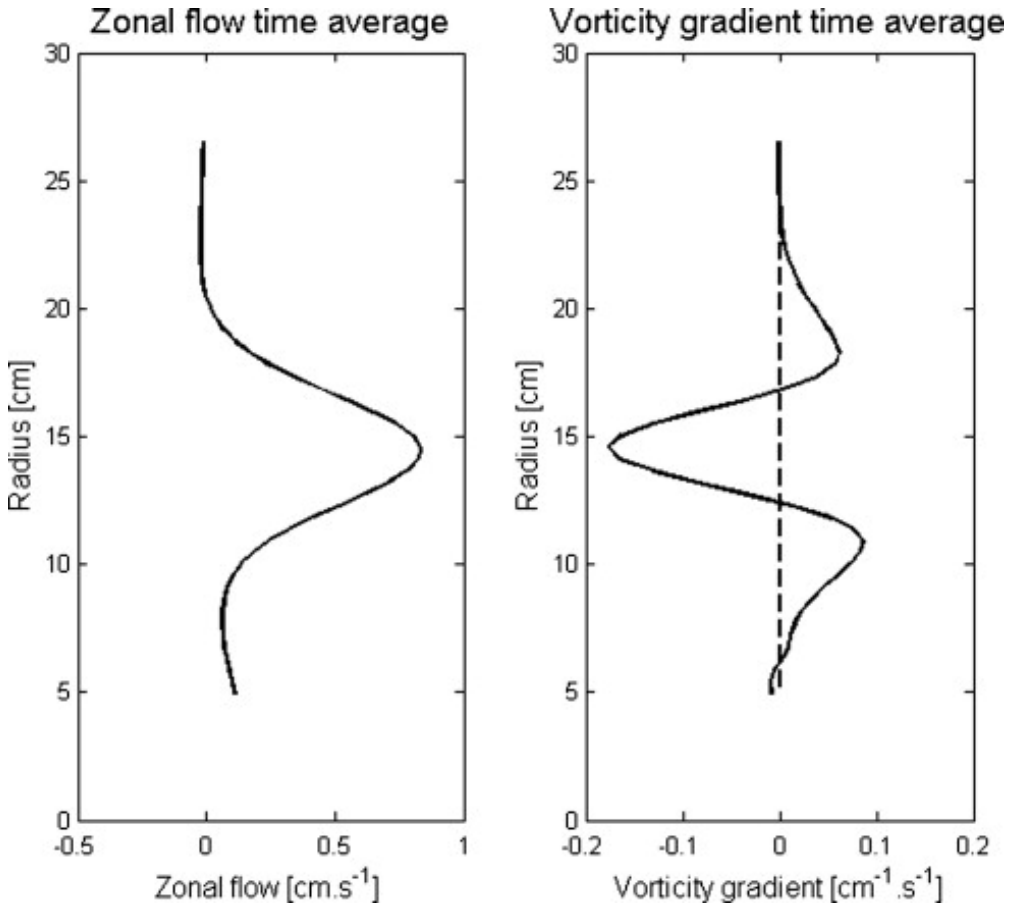

FIG. 9: The mean zonal velocity (left) and vorticity gradient (right) as measured from analysis of flow images in laboratory experiments using the ring setup. On the right, $\beta = 0$ corresponds to the dashed line, and violation of the Rayleigh-Kuo criterion is evident. Also, note how the profiles appear similar to the observed Saturnian hexagon's profile in Figure 7 [1, fig 6].

either be a disk in contact with both the top and bottom of the fluid or a ring in contact with only the upper fluid surface, and its differential rotation forces out a jet-like flow from the body fluid [1]. A non-zero β parameter could be simulated by conical bottoms sloping away from the center. The results for both setups are shown in Figure 6, and their measured mean zonal flow velocities and vorticity gradients are shown in Figure 9. These appear similar to the profiles observed for Saturn's hexagon, and violation of the Rayleigh-Kuo criterion occurs on either side of the jet flow [1].

Additionally, a numerical simulation based on the Explicit Planetary Isentropic-Coordinate (EPIC) model demonstrated the possible formation of stable polygons as a result of insta-

bilities arising from zonal jet nonlinear equilibrations [12]. They found that the zonal wave number depended strongly on u_{yy}, as speculated in previous studies. By initially seeding the simulation with a Gaussian velocity profile, polygons formed and propagated with velocities given by the Rossby wave dispersion relation, as suggested years earlier by Allison et al. [2, 12]. However, their simulated propagation rate did not match the hexagon's observed rotation. A modified initial velocity profile was developed, with an additional term that "slowed down" the wave propagation [12]. The simulated jets violated the Rayleigh-Kuo criterion, and the dominant instability mode was speculated to be barotropic instabilities in agreement with the Barbosa Aguiar experiment discussed above [12].

VII. CONCLUSION

Although the exact cause behind Saturn's north polar hexagon still remains somewhat of a mystery, much progress has been made since its initial discovery to allow a better understanding of a startling phenomena. Starting with Voyager and Godfrey's initial discovery, the hexagon first appeared alongside an impinging vortex, with a near zero rotation rate relative to Saturn's radio rotation period [9]. Images from the HST and Pic-du-Midi observatory in the early 90s confirmed both facts over ten years later [5, 15]. The images from Voyager bedazzled and baffled scientists, and many early hypotheses as to the cause of the stationary wave were speculated. The most realistic of them, forcing from below due to internal convective heating, was propounded by both Godfrey and Gierasch [7, 9], but it wasn't until the Rossby wave theory that a mathematical description of the nature of the hexagon was given [2]. With the Cassini mission entering into orbit in 2004, interest in Saturn's hexagon was revived. It was discovered that the impinging vortex no longer existed, thus refuting the perturbative Rossby wave theory given by Allison et al. [3]. Laboratory experiments demonstrated the possibility of spontaneous polygonal formation in rotating fluids, with the cause attributed to barotropic instabilities arising in the zonal jet flows surrounding the polygons [1, 11, 12]. The laboratory analogue were found to have zonal flows and vorticity gradients comparable to those observed on Saturn, and is probably the best explanation of Saturn's hexagon we have today.

Appendix: Fluid Dynamics in Brief

The following is a summary of some chapters from Pedlosky's *Geophysical Fluid Dynamics* [13], Batchelor's *An Introduction to Fluid Mechanics* [4], and Gill's *Atmosphere-Ocean Dynamics* [8].

A fluid flow is, at the most fundamental level, described by a *velocity field*, $\mathbf{u}$. In the Eulerian methodology, this requires a velocity vector to be assigned at every point in the space of the fluid [4]. It is then of interest to attack the problem of the time evolution the velocity field,

$$\frac{d\mathbf{u}}{dt} = \frac{\partial \mathbf{u}}{\partial t} + \mathbf{u} \cdot (\nabla \mathbf{u}). \tag{A.1}$$

The continuity equation, along with conservation laws, gives an equation of motion for $\mathbf{u}$ in a non-rotating frame [13]. In a rotating frame, the equation of motion is modified by the Coriolis acceleration to be,

$$\rho \left[\frac{d\mathbf{u}}{dt} + 2\boldsymbol{\Omega} \times \mathbf{u} \right] = -\nabla p + \rho \nabla \Phi + \mathcal{F}, \tag{A.2}$$

where the density ρ has been assumed constant, $\boldsymbol{\Omega}$ is the planetary rotation, p the pressure, Φ is the modified potential due to gravity and centripedal acceleration, and $\mathcal{F}$ is any additional frictional force [13]. From Equation A.2, we see that the Coriolis acceleration contributes a factor of $2\boldsymbol{\Omega} \times \mathbf{u}$, estimated as $O(2\Omega U)$. Taking the ratio of the relative acceleration $\frac{d\mathbf{u}}{dt} \approx O(U^2/L)$ to the Coriolis acceleration gives the important *Rossby number* $\epsilon = \frac{U}{2\Omega L}$ [4, 13]. The Rossby number is an estimate of the relative importance of the Coriolis force on the velocity field. For small Rossby number, the Coriolis acceleration is important. This is the case for large scale flows such as Saturn's hexagon as the relative acceleration becomes small in comparison to the Coriolis acceleration.

Given a velocity field, it is useful to define the *vorticity* as $\boldsymbol{\omega} = \nabla \times \mathbf{u}$ and work with equations of motion in terms of the vorticity instead [4, 13]. Note that there is a direct analogy between the relationship of vorticity and velocity field to that of the current density and magnetic field. However, there is no causal relationship in the case of vorticity and velocity field; the vorticity is simply a useful and intuitive concept for understanding fluid flows. The planetary vorticity is $2\boldsymbol{\Omega}$ and the component of the planetary vorticity normal to the planet's surface is called the Coriolis parameter [13],

$$f = 2\Omega \sin\theta. \tag{A.3}$$

By treating a thin latitudinal strip on a sphere as a geometrically flat plane, f can be linearly approximated as $f \approx f_0 + \beta_0 y$, where $f_0 = 2\Omega \sin\theta_0$ and $\beta_0 = \frac{2\Omega}{r_0}\cos\theta_0$ [13]. This is called the β-plane approximation, and is used extensively in atmospheric models, including that of Saturn's hexagon.

In a rotating reference frame, the absolute vorticity is defined as $\boldsymbol{\omega_a} = \boldsymbol{\omega} + 2\boldsymbol{\Omega}$, the sum of relative and planetary vorticities. Starting with Equation A.2, it is possible to derive the vorticity equation [13]:

$$\frac{d\boldsymbol{\omega}}{dt} = \boldsymbol{\omega_a} \cdot \nabla \mathbf{u} - \boldsymbol{\omega_a} \nabla \cdot \mathbf{u} + \frac{\nabla\rho \times \nabla p}{\rho^2} + \nabla \times \frac{\mathcal{F}}{\rho}. \tag{A.4}$$

The third term on the right hand side is called the baroclinic vector. A fluid is baroclinic if $\frac{\nabla\rho\times\nabla p}{\rho^2} \neq 0$, and barotropic otherwise. A barotropic fluid thus by definition must have coinciding surfaces of constant ρ and p, and a relation $\rho = \rho(p)$ can be found [13]. Instabilities that arise in both barotropic and baroclinic fluids play a crucial role in large scale flow dynamics and the wave patterns that arise in planetary atmospheres. Several theoretical descriptions of the Saturnian north polar hexagon use instability theory as a starting point in modeling its dynamical behavior.

Finally, one can define the potential vorticity as

$$\Pi = \frac{\boldsymbol{\omega_a}}{\rho} \cdot \nabla\lambda, \tag{A.5}$$

where λ is some property such as density or the potential temperature [13]. The potential vorticity is a useful concept as it allows vertical structure to be incorporated via the parameter λ for three dimensional fluids. It is conserved under the following conditions:

- the fluid is barotropic or λ is dependent on only ρ and p,
- λ is conserved for each fluid element,
- the frictional force is negligible [13].

---

[1] Ana C. Barbosa Aguiar, Peter L. Read, Robin D. Wordsworth, Tara Salter, and Y. Hiro Yamazaki. A laboratory model of Saturn's north polar hexagon. *Icarus*, 206(2):755 – 763, 2010. Cassini at Saturn.

[2] M. Allison, D. A. Godfrey, and R. F. Beebe. A wave dynamical interpretation of Saturn's polar hexagon. *Science*, 247(4946):1061–1063, 1990.

[3] Kevin H. Baines, Thomas W. Momary, Leigh N. Fletcher, Adam P. Showman, Maarten Roos-Serote, Robert H. Brown, Bonnie J. Buratti, Roger N. Clark, and Philip D. Nicholson. Saturn's north polar cyclone and hexagon at depth revealed by cassini/vims. *Planetary and Space Science*, 57(1415):1671 – 1681, 2009.

[4] G.K. Batchelor. *An Introduction to Fluid Mechanics*. Cambridge University Press, 1967.

[5] John Caldwell, Benoit Turgeon, Xin-Min Hua, Christopher D. Barnet, and James A. Westphal. The Drift of Saturn's North Polar Spot Observed by the Hubble Space Telescope. *Science*, 260(5106):326–329, 1993.

[6] L. N. Fletcher, P. G. J. Irwin, G. S. Orton, N. A. Teanby, R. K. Achterberg, G. L. Bjoraker, P. L. Read, A. A. Simon-Miller, C. Howett, R. de Kok, N. Bowles, S. B. Calcutt, B. Hesman, and F. M. Flasar. Temperature and composition of saturn's polar hot spots and hexagon. *Science*, 319(5859):79–81, 2008.

[7] Peter J. Gierasch. Hexagonal polar current on Saturn. *Nature*, 337(6205):309, 1989.

[8] Adrian Gill. *Atmosphere-Ocean Dynamics*. Academic Press, 1982.

[9] D. A. Godfrey. A hexagonal feature around Saturn's north pole. *Icarus*, 76(2):335 – 356, 1988.

[10] D. A. Godfrey. The rotation period of Saturn's polar hexagon. *Science*, 247(4947):1206–1208, 1990.

[11] Thomas R. N. Jansson, Martin P. Haspang, Kåre H. Jensen, Pascal Hersen, and Tomas Bohr. Polygons on a rotating fluid surface. *Phys. Rev. Lett.*, 96:174502, May 2006.

[12] Raul Morales-Juberias, Kunio M. Sayanagi, Timothy E. Dowling, and Andrew P. Ingersoll. Emergence of polar-jet polygons from jet instabilities in a saturn model. *Icarus*, 211(2):1284 – 1293, 2011.

[13] Joseph Pedlosky. *Geophysical Fluid Dynamics*. Springer-Verlag, 2nd edition, 1987.

[14] R. Alan Plumb. Rossby waves and planetary scale motions. MIT Course Notes. `http://www-eaps.mit.edu/~rap/courses/12333_notes/Chap5.pdf`.

[15] A. Sanchez-Lavega, J. Lecacheux, F. Colas, and P. Laques. Ground-based observations of saturn's north polar spot and hexagon. *Science*, 260(5106):329–332, 1993.

[16] J. Trauger. Astronomy picture of the day, December 2001. `http://apod.nasa.gov/apod/ap011223.html`.